AD-A058 588 NAVAL RESEARCH LAB WASHINGTON D C F/G 18/13
STRUCTURAL INTEGRITY OF WATER REACTOR PRESSURE BOUNDARY COMPONE--ETC(U)
MAY 78 F J LOSS AT(49-24)-0207
UNCLASSIFIED NRL-MR-3782 SBIE-AD-E000 204 NL

1 OF 1
AD
A058588

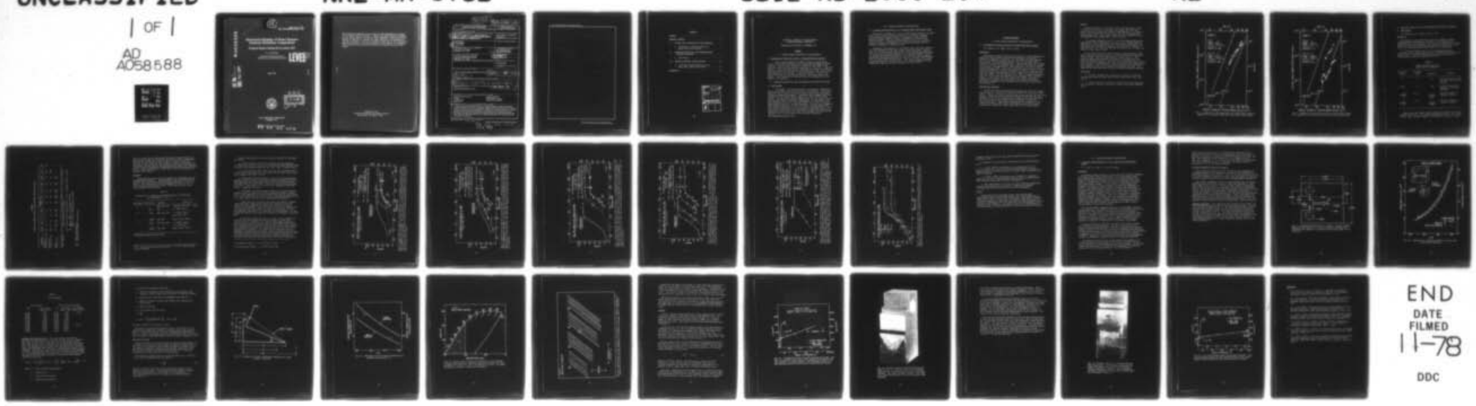

END
DATE
FILMED
11-78
DDC

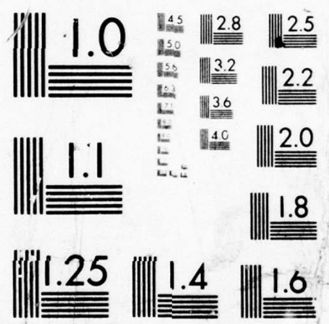

MICROCOPY RESOLUTION TEST CHART

NATIONAL BUREAU OF STANDARDS-1963-A

NRL Memorandum Report 3782

Structural Integrity of Water Reactor Pressure Boundary Components

Progress Report Ending 30 November 1977

F. J. Loss, Editor

Thermostructural Materials Branch
Material Science and Technology Division

May 1978

NAVAL RESEARCH LABORATORY
Washington, D.C.

Available from
National Technical Information Service
Springfield, Virginia 22161

18 SBIE

19 AD-E000 204

SECURITY CLASSIFICATION OF THIS PAGE (When Data Entered)

REPORT DOCUMENTATION PAGE		READ INSTRUCTIONS BEFORE COMPLETING FORM
1. REPORT NUMBER NRL Memorandum Report 3782	2. GOVT ACCESSION NO.	3. RECIPIENT'S CATALOG NUMBER
4. TITLE (and Subtitle) 6 STRUCTURAL INTEGRITY OF WATER REACTOR PRESSURE BOUNDARY COMPONENTS, ~~PROGRESS REPORT ENDING 30 NOVEMBER 1977~~		5. TYPE OF REPORT & PERIOD COVERED Interim report on a continuing NRL problem.
		6. PERFORMING ORG. REPORT NUMBER
7. AUTHOR(s) 10 F.J. Loss, Editor		8. CONTRACT OR GRANT NUMBER(s)
9. PERFORMING ORGANIZATION NAME AND ADDRESS Naval Research Laboratory Washington, D.C. 20375		10. PROGRAM ELEMENT, PROJECT, TASK AREA & WORK UNIT NUMBERS 15 NRL Problem M01-40 Project AT(49-24)-0207
11. CONTROLLING OFFICE NAME AND ADDRESS U.S. Nuclear Regulatory Commission Division of Reactor Safety Research Washington, D.C. 20555		12. REPORT DATE 11 May 1978
		13. NUMBER OF PAGES 37
14. MONITORING AGENCY NAME & ADDRESS (if different from Controlling Office)		15. SECURITY CLASS. (of this report) UNCLASSIFIED
		15a. DECLASSIFICATION DOWNGRADING SCHEDULE

16. DISTRIBUTION STATEMENT (of this Report)

Approved for public release; distribution unlimited. 14 NRL-MR-3782

12 37 p.

17. DISTRIBUTION STATEMENT (of the abstract entered in Block 20, if different from Report)

9 Progress rept. for period ending 30 Nov 77,

18. SUPPLEMENTARY NOTES

Distribution includes NRC-1 and 5.

19. KEY WORDS (Continue on reverse side if necessary and identify by block number)

Nuclear pressure vessel steels
J-integral
Low upper shelf
Charpy-V test
Radiation sensitivity
Post-irradiation recovery
Fatigue crack propagation

20. ABSTRACT (Continue on reverse side if necessary and identify by block number)

This report describes research progress in a continuing program to characterize materials properties performance with respect to structural integrity of light water reactor pressure boundary components. Progress for this reporting period is summarized in the following areas: (a) evaluation of critical factors in crack growth rate studies in a pressurized water reactor environment, (b) irradiation and postirradiation (annealing) heat treatment study of the toughness of pressure vessel steels having a low upper shelf level; and (c) J integral characterization of an A302B steel having a low upper shelf energy.

DD FORM 1 JAN 73 1473 EDITION OF 1 NOV 65 IS OBSOLETE
S/N 0102-014-6601

SECURITY CLASSIFICATION OF THIS PAGE (When Data Entered)

78 08 09 090

251 950

SECURITY CLASSIFICATION OF THIS PAGE (*When Data Entered*)

SECURITY CLASSIFICATION OF THIS PAGE(*When Data Entered*)

CONTENTS

SUMMARY. 1

RESEARCH PROGRESS. 3

I. FATIGUE CRACK PROPAGATION IN LWR MATERIALS . . . 3

A. Evaluation of Critical Factors in Crack Growth Rate Studies 3

II. RADIATION SENSITIVITY AND POSTIRRADIATION PROPERTIES RECOVERY. 7

A. IAR Program. 7

III. FRACTURE MECHANICS INVESTIGATIONS. 18

A. J-Integral Characterization of Low Upper Shelf A302-B Steel Plate 18

REFERENCES 34

STRUCTURAL INTEGRITY OF WATER REACTOR
PRESSURE BOUNDARY COMPONENTS

PROGRESS REPORT ENDING 30 NOVEMBER 1977

SUMMARY

I. FATIGUE CRACK PROPAGATION IN LWR MATERIALS

A. Evaluation of Critical Factors in Crack Growth Rate Studies

Cyclic crack growth rate (CCGR) testing was continued in accord with the NRC preliminary matrix using 1TCT specimens of A508-2 forging. A previous test indicated a relatively high CCGR in the water pot with a loading waveform consisting of 1 min ramp - 3 min hold periods. A duplicate test has now confirmed this trend. An identical high growth rate was exhibited by another water pot test having a waveform consisting of 5 min ramp - 1 min hold periods. A test of the latter wave form in an autoclave produced a much lower growth rate, however. This result was not expected and an investigation of this behavior is continuing.

II. RADIATION SENSITIVITY AND POSTIRRADIATION PROPERTIES RECOVERY

A. IAR Program

Experiment 2 of the IAR program, containing two submerged arc welds and an A302-B (modified) plate has been completed. The primary objective was to explore C_v notch ductility trends with irradiation-anneal-reirradiation treatments. Annealing heat treatments evaluated included a 343°C (650°F)-168 hr anneal and a 399°C (750°F)-168 hr anneal. The exploratory results suggest that, for the irradiation and reirradiation fluence conditions investigated, an intermediate 343°C heat treatment may not be a practical method for control of neutron embrittlement because of the high frequency of reactor vessel annealing which would be required. On the other hand, an intermediate 399°C heat treatment does appear to be an effective annealing method. Full upper shelf recovery but not full transition temperature recovery was achieved for both welds by the 399°C heat treatment procedure following both first cycle and second cycle radiation exposures.

Note: Manuscript submitted May 2, 1978.

III. FRACTURE MECHANICS INVESTIGATIONS

A. J Integral Characterization of Low Upper Shelf A302-B Steel Plate

The fracture toughness of a plate of A302-B steel having a low upper shelf energy is being investigated with the J integral procedure. Special emphasis has been placed on development of the unloading compliance method (UCM) as a means to evolve the J-R curve with a single specimen. A demonstrated UCM capability by remote testing is required to assess the toughness of irradiated materials that are generally available in limited quantity.

Preliminary investigations of the A302-B steel have been conducted with 1TCT specimens in the upper shelf temperature regime. Results point out an error between the specimen crack extension determined by the UCM and by optical measurements of the fracture surface. The use of face-grooved specimens eliminates the "tunneled" crack extension exhibited by the smooth specimens but does not eliminate the preceding error in crack length determination. The R curve slope of the face-grooved specimens is less than that of the smooth specimens, thereby suggesting a specimen geometry dependence of the R curve.

RESEARCH PROGRESS

I. FATIGUE CRACK PROPAGATION IN LWR MATERIALS

A. Evaluation of Critical Factors in Crack Growth Rate Studies

H.E. Watson, B.H. Menke, and F.J. Loss

Background

Experimental results discussed here pertain to tests continuing in support of the preliminary test matrix developed by the Nuclear Regulatory Commission to simulate: (a) the hydro and leak transient, (b) the heat up and cooldown transient, and (c) the steady state operation of a nuclear pressure vessel. The primary objective of these tests is to define the important test variables to be used in the main test program. Specimens used in these tests are 25 mm (1-in.) thick compact toughness (CT). Tests were conducted using an R-ratio of 0.125 and loading waveforms aimed at evaluating the effect of hold and rise times on fatigue crack propagation (FCP). Results are presented from autoclave (288°C, 13.8 MPa) and water pot (93°C, atmospheric pressure) tests and crack length measurements are determined by the compliance method. In all cases, the crack growth rate, da/dN, values are determined by computer analysis using the incremental polynominal technique recommended by the ASTM Task Group on Fatigue Crack Growth Rate Testing (1).

Experimental Procedure

The FCP data were generated using autoclave and water pot fatigue test equipment to simulate the heatup and hydro/leak transients respectively. The water chemistry specification (2) for the two test systems is identical except for gas concentration resulting from the cover gas. Hydrogen is used in the autoclave and nitrogen in the water pot tests. The water is circulated through both test chambers to maintain a uniform chemistry. Crack length measurements are referenced to the crack mouth opening (CMO) and are determined using linear variable differential transformers (LVDT) which operate in the environment.

Results

Previous results (3) combining a 1-min. rise time with a 3 min. hold period in the water pot produced the highest FCP rates ever observed at NRL for tests using A508-2 forging material. To obtain a higher level of confidence in that data, this test was duplicated using specimen FW-7. The results of that test are presented in Fig. 1 and compared to the earlier data. (FW-7 vs FW-14).

In an earlier progress report (3), data from specimen FW-14 have been compared with a recent water pot test using a loading waveform composed of a 5-min. ramp and a 1-min. hold period (Spec. FW-8). The data trends were essentially identical indicating that changing the ramp time from 1 to 5 min. and the hold time from 1 min. to 3 min. had little, if any, effect on FCP.

An autoclave test (Spec. FW-13) has been completed with a 5-min. ramp, 1-min hold period to compare with the water pot test conducted earlier (FW-8). Data from both tests are shown in Fig. 2. The autoclave result was unexpected since most of the data fell on or below the ASME Section XI air line, whereas in previous tests, for a given set of test conditions, the water pot and autoclave tests compared very favorably. The difference in these data cannot be attributed to water chemistry since it was comparable throughout each test. The cause of the large variation in these two tests is being investigated.

Conclusion

1. The FW-7 specimen test confirmed the validity of high FCP data obtained from the FW-14 using a 1-min. ramp with a 3-min. hold period.

2. Further tests are necessary to explain the large differences that occurred in the FW-13 (autoclave) and FW-8 (water pot) specimen tests.

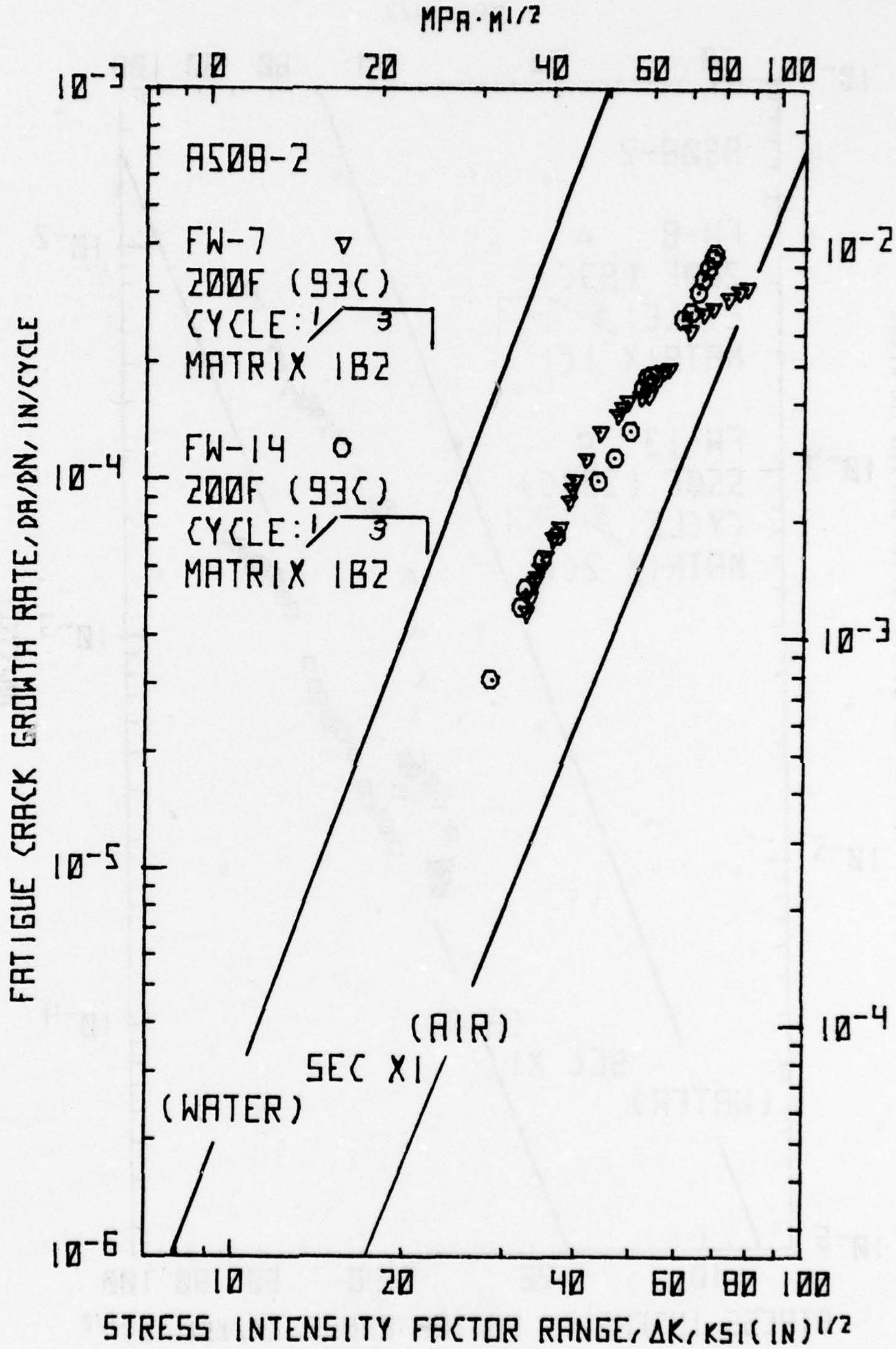

Fig. 1 - Comparison of duplicate water pot tests using a waveform composed of a one minute ramp and a three minute hold period.

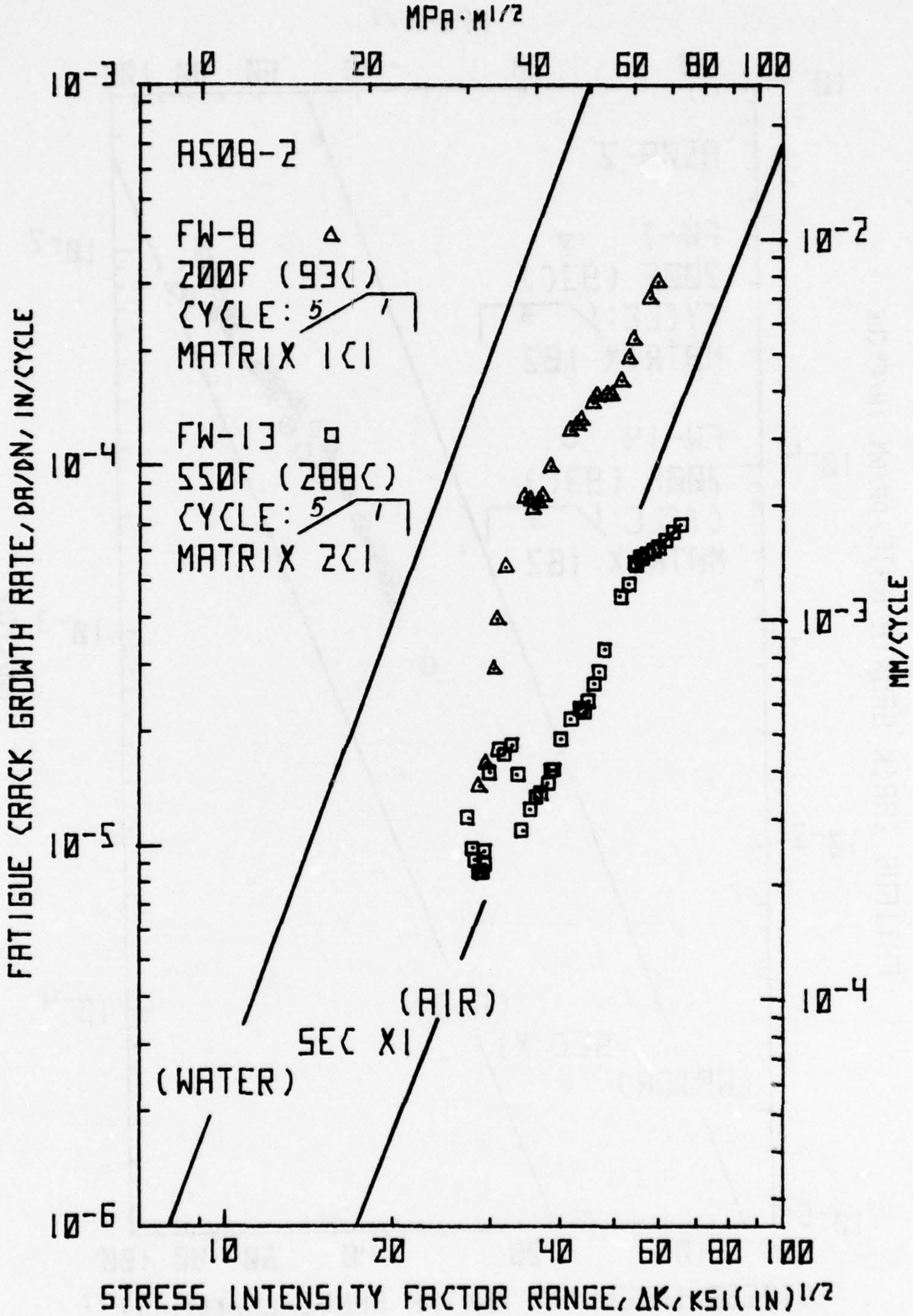

Fig. 2 - Comparison of autoclave and water pot tests using a waveform composed of a five minute ramp and a one minute hold period.

II. RADIATION SENSITIVITY AND POSTIRRADIATION PROPERTIES RECOVERY

A. IAR Program

J.R. Hawthorne, H.E. Watson, and F.J. Loss

Background

The initials of the IAR Program stand for "Irradiate, Anneal, and Reirradiate" respectively. The intent of the program is to investigate material performance under two full annealing and reirradiation cycles such that the merits and potential of the method of the control of radiation-induced embrittlement can be identified.

In a previous progress report (4), the background and the objectives of the program were outlined. The planned experimental test matrix (Table 1) was also discussed together with a description of the materials selected for study (Table 2) (3).

Table 1

Radiation Experiment Matrix
288°C (550°F) Irradiation

Experiment Number	Specimen Types	Designation	Objective
1	C_v	IA	Explore recovery by 343 and 399°C (650 and 750°C) annealing
2 A,B,C	C_v	IAR	Explore reirradiation response of all three materials
3A through 3E	CT, C_v	I through IARAR	Determine IARAR performance of Weld 1
4A through 4E	CT, C_v	I through IARAR	Determine IARAR performance of Weld 2

Results from Experiment 1 were presented and analyzed in the last progress report (3). Two important determinations were: (a) a 343°C-168 hour heat treatment achieved a high degree of recovery in upper

Table 2

CHEMICAL COMPOSITIONS OF IARAR PROGRAM WELDS AND PLATE

MATERIAL	CODE		Weight (%) Cu	C	Mn	Si	P	S	Ni	Mo	V	Cr
S/A Weld 1 (Linde 1092 flux)	V84	(a)	.35	.14	1.56	.14	.013	.011	.62	.53	.002	.03
S/A Weld 2 (Linde 80 flux)	V86	(a)	.35	.08	1.60	.55	.016	.013	.69	.40	.006	-
Plate 1 (A302-B Mod.)	V85	(a)	.22	.22	1.50	.27	.013	.020	.53	.46	-	-
		(b)	.24	.22	1.45	.30	.011	.014	.52	.48	-	-

Heat Treatment	V84	Stress relief annealed 593 to 621°C - 50 hr, furnace cooled to 316°C at 6°C/hr, air cooled.
	V86	Stress relief annealed 621°C - 40 hr, furnace cooled to 316°C.
	V85	843 to 899°C - 4 hr, water quenched 663°C - 4 hr, air cooled 621°C - 40 hr, furnace cooled to 316°C

(a) Vendor determination
(b) Lukens Steel Company determination

shelf for welds V84 and V86 (62 and 100 percent, respectively), but only limited recovery in transition (29 and 22 percent, respectively) whereas, (b) a 399°C-168 hr heat treatment produced 100 percent recovery in upper shelf and ∿70 percent in transition temperature for both welds. On the basis of these findings, the target reirradiation fluence (ϕ^{fs*}) for Experiment 2B (IAR with 343°C anneal) was established at 3×10^{18} n/cm^2 and at 6×10^{18} n/cm^2 >1 MeV for Experiment 2C IAR with 399°C anneal).

Progress

Postirradiation testing and data analyses for Experiments 2A, B, C have now been completed. The experiments each contained welds V84 and V86 and plate V85 and provided material conditions as listed in Table 3. The experimental data are presented in Figs. 3 to 7. It should be noted that fluences (n/cm^2 >1 MeV) given in each figure are preliminary estimates only.

Table 3

Irradiation (I), Anneal (A), and Reirradiation (R) Conditions of Experiments 2 A, B, C

Experiment	Description	Material	Condition†
A	I	V84, V85, V86	1.2×10^{19} n/cm^2 (ϕ^{cs} >1 MeV)
	IA_2	V86	I + 399°C -168 hr
B	IA_1R	V84, V85, V86	I + 343°C -168 hr + 3.6×10^{18} n/cm^2
	IA_1RA_1	V84, V86	IA_1R + 343°C -168 hr
C	IA_2R	V84, V85, V86	I + 399°C -168 hr + 7.2×10^{18} n/cm^2
	IA_2RA_2	V84, V86	IA_2R + 399°C -168 hr

† Preliminary fluence values (ϕ^{cs}).

*ϕ^{cs} >1 MeV (calculated spectrum fluence) = 1.2 ϕ^{fs} >1 MeV (fission spectrum fluence)

Several observations can be made from the results for the welds as follows:

1. Notch ductility after 343^{o}C annealing and reirradiation* is either poorer than or the same as the notch ductility observed after the first cycle radiation exposure (see Figs. 3 and 5, respectively).

2. Notch ductility after 399^{o}C annealing and reirradiation** is better than the notch ductility observed after the first cycle irradiation exposure (see Figs. 4 and 6).

3. The amount of reembrittlement produced by the reirradiation exposure alone, in terms of transition temperature change, is greater than that projected for non-heat treated material whose fluence is increased from 1.2 x 10^{19} n/cm^2 to the final (cycle 1 plus 2) fluence value (i.e., 1.56 n/cm^2 or 1.92 x 10^{19} n/cm^2, depending on the IAR versus I comparison involved.

4. The amount of reembrittlement produced by the reirradiation exposure alone, in terms of transition temperature change, is about equal to that projected for virgin material receiving the same fluence (i.e., 3.6 x 10^{18} n/cm^2 in the case of the 343^{o}C annealed material, or 7.2 x 10^{18} n/cm^2 in the case of the 399^{o}C annealed material).

5. Notch ductility following the second cycle anneal treatment (IARA condition), judging from limited data available, is either equal to or better than that produced by the first cycle anneal treatment (IA condition). With reference to the earlier assessments, good agreement was found between the notch ductility data for the as-irradiated conditions (I) of Experiment 2 and Experiment 1 (3) and between the data for the respective irradiated and annealed conditions (IA).

In the case of plate V85 (Fig. 7), only a few specimens were available from each experiment and were assigned to upper shelf condition tests. Analysis of the results were somewhat hampered by data scatter; however, it appears that the upper shelf level of the 399^{o}C annealed and reirradiated condition (but not the 343^{o}C annealed and reirradiated condition) is higher than that for the first cycle irradiated (I) condition. This indication is consistent with the findings for the weld deposits above. Figure 8 compares data for the unirradiated plate developed independently by NRL and two other sites. The notch ductility variation, which stem from the evaluation of different plate sections, demonstrates well the need for generating

---

*reirradiation fluence: 3.6 x 10^{18} n/cm^2 >1 MeV

** reirradiation fluence: 7.2 x 10^{18} n/cm^2>1 MeV

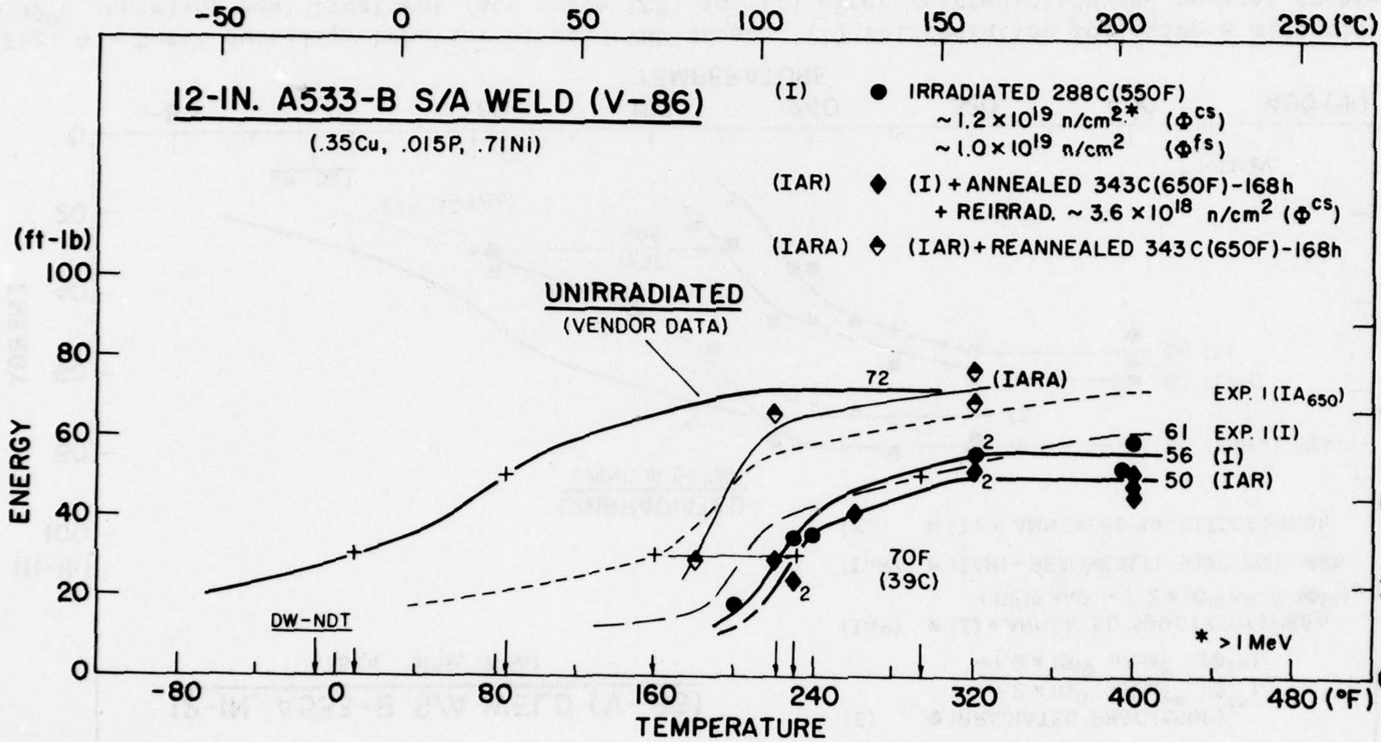

Fig. 3 - Notch ductility behavior of weld V86 after: (1) reirradiation following a midcycle 343°C annealing heat treatment (see curve IAR), and (2) after reirradiation and reheat treatment at 343°C (see curve IARA). The notch ductility of the weld after the first cycle irradiation (curve I) and after the first cycle heat treatment (approximated by curve 1A of Exp. 1) are also shown for reference.

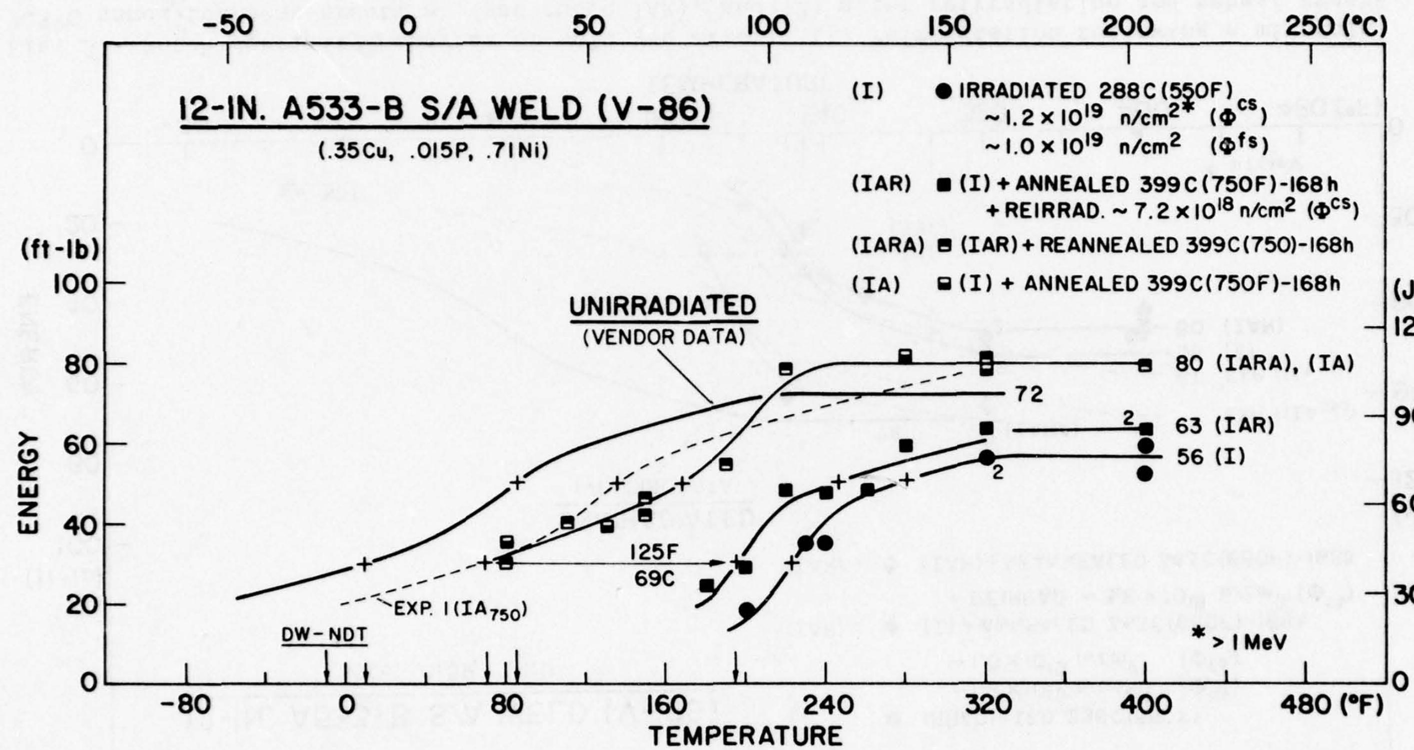

Fig. 4 - Notch ductility behavior of weld V86 after: (1) reirradiation following a midcycle 399°C annealing heat treatment (see curve IAR) and (2) after reirradiation and re-heat treatment at 399°C (see curve IARA). The notch ductility of the weld after the first cycle irradiation (curve I) and after the first cycle heat treatment (see data points IA) are also shown for reference.

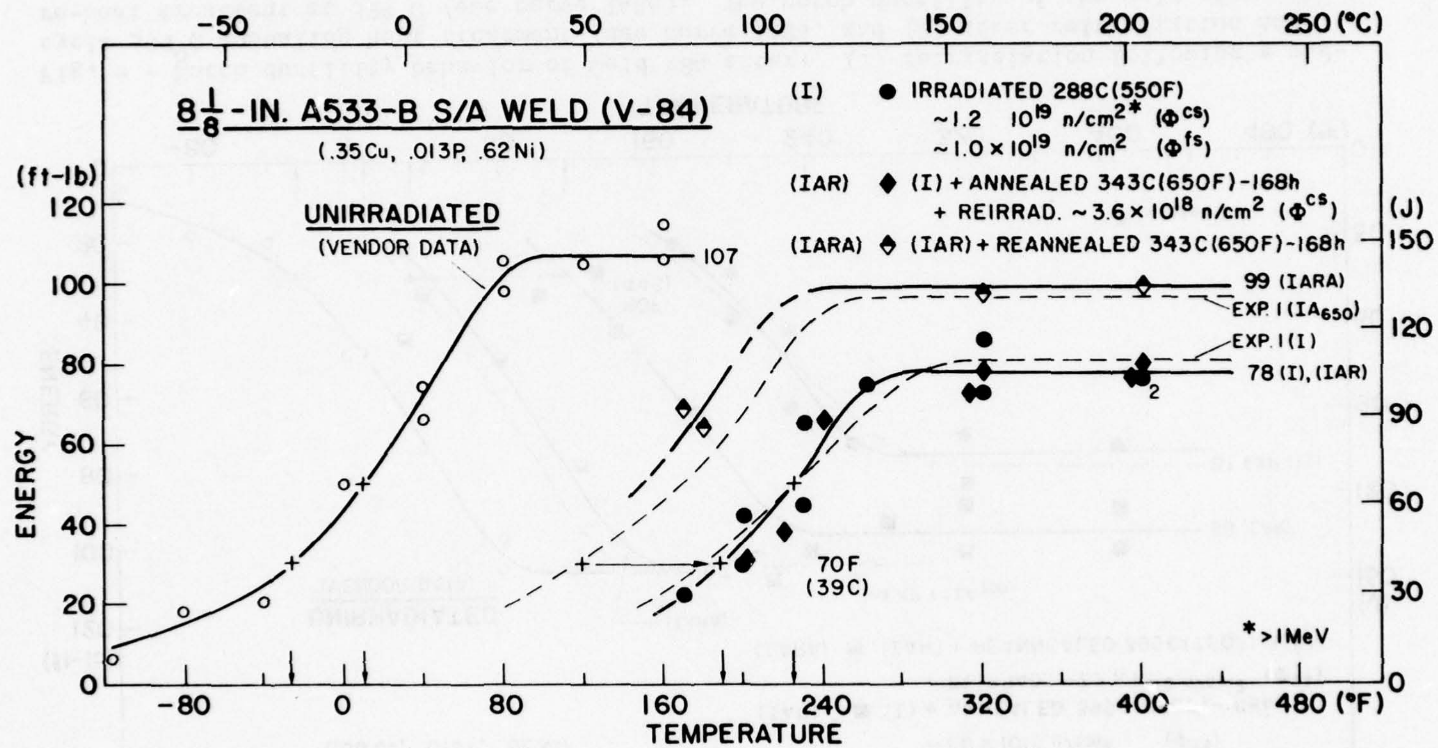

Fig. 5 - Notch ductility behavior of weld V84 after: (1) reirradiation following midcycle 343°C annealing heat treatment (see curve IAR), and (2) after reirradiation and re-heat treatment of 343°C (see curve IARA). The notch ductility of the weld after the first cycle irradiation (curveI) and after the first cycle heat treatment (approximated by curve IA of Exp. 1) are also shown for reference.

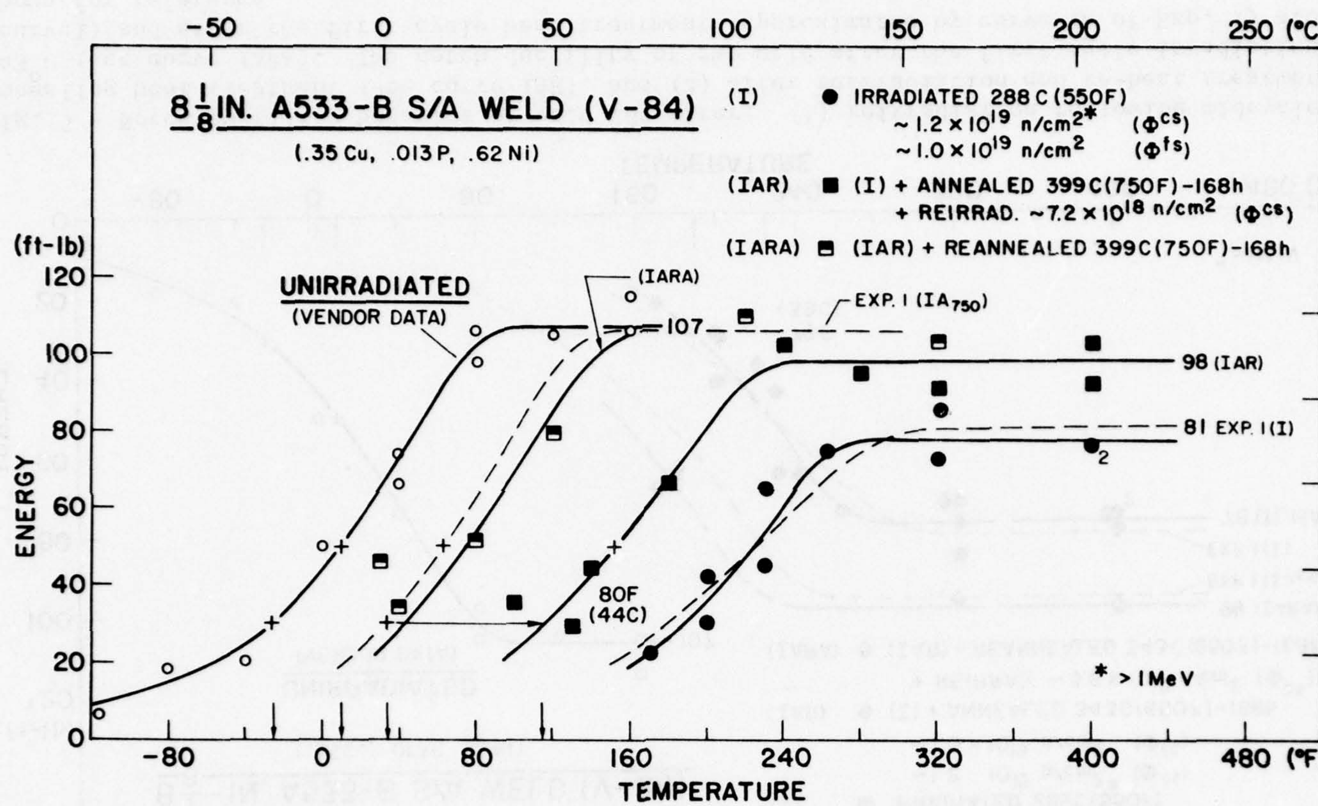

Fig. 6 - Notch ductility behavior of weld V84 after: (1) reirradiation following a mid-cycle 399°C annealing heat treatment (see curve IAR), and (2) after reirradiation and re-heat treatment at 399°C (see curve IARA). The notch ductility of the weld after the first cycle irradiation (curve I) and after the first cycle heat treatment (approximated by curve IA of Exp. 1) are also shown for reference.

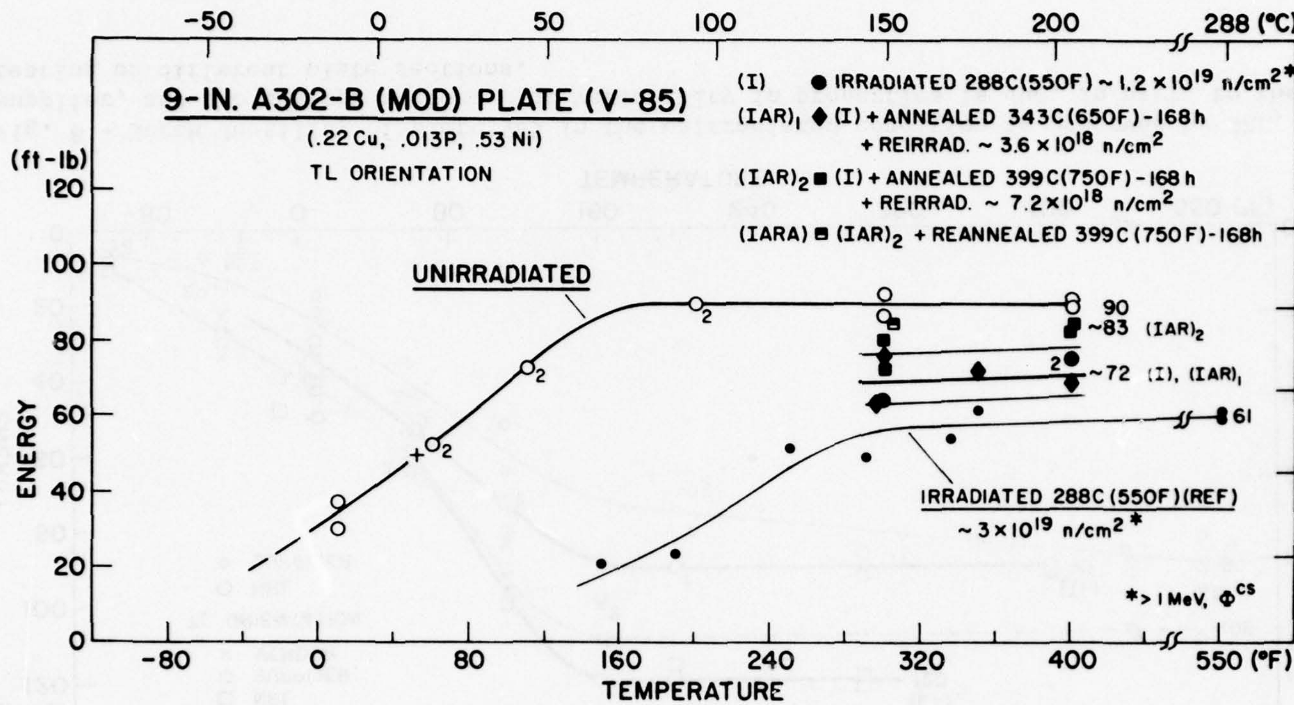

Fig. 7 - Upper shelf notch ductility of plate V85 after first cycle irradiation (I), after reirradiation following a midcycle 343°C annealing heat treatment $(IAR)_1$, and alternatively, after reirradiation following a midcycle 399°C annealing heat treatment $(IAR)_2$. The upper shelf level of the reirradiated condition $(IAR)_2$, but not reirradiation condition $(IAR)_1$, appears somewhat higher than that of the upper shelf level of the as-irradiated condition (I). Results for a high fluence assessment of the plate (prior study) are also shown.

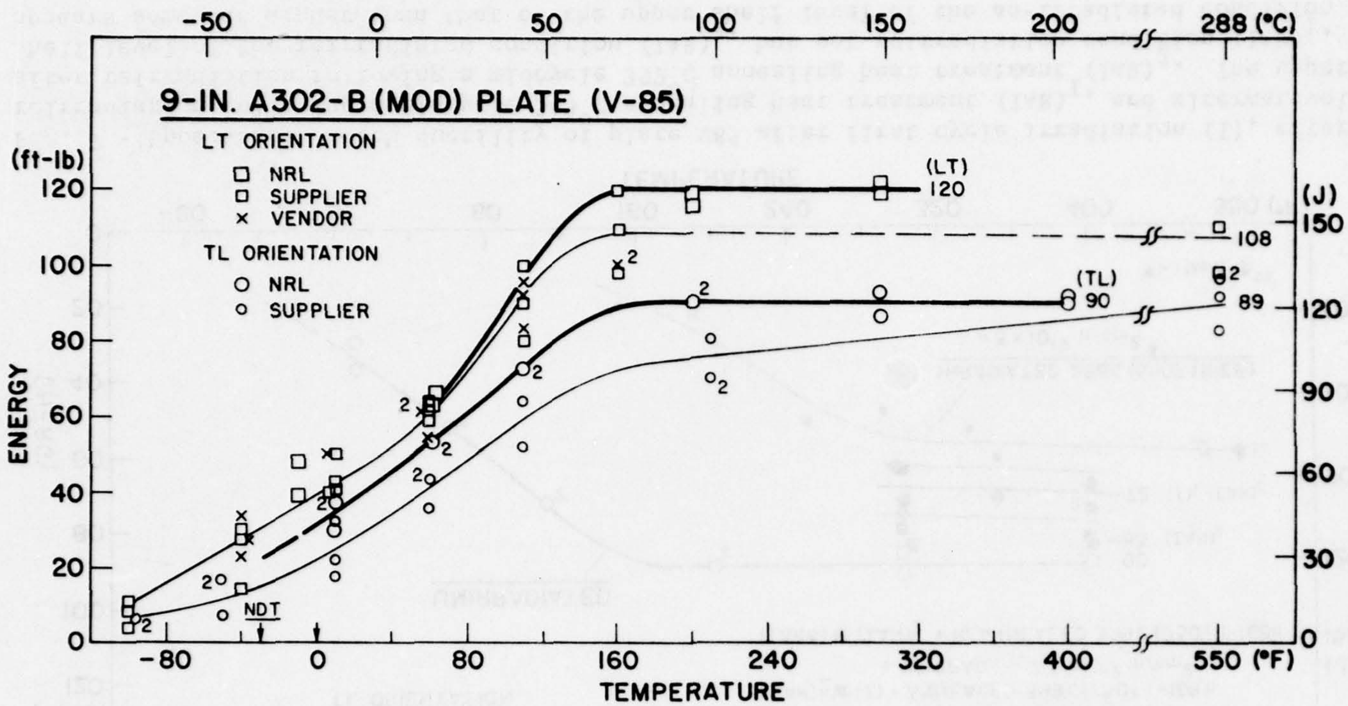

Fig. 8 - Notch ductility of plate V85 in the unirradiated condition as observed by NRL, the supplier, and the reactor vendor. The variability in properties is due, in part, to the testing of different plate sections.

reference condition data for that same location in the plate used for irradiation tests.

To summarize the experimental observations, the results indicate that:

1. A 343°C (650°F) intermediate heat treatment may not be a practical method for control of radiation embrittlement in reactor vessels because of the high frequency of reactor vessel annealing which would be required.

2. A 399°C (750°F) intermediate heat treatment is a promising method for control of radiation embrittlement for the irradiation and heat treatment conditions of present investigation.

3. Full upper shelf recovery but not full transition temperature recovery was developed in both welds by a 399°C heat treatment following first cycle and second cycle radiation exposures.

<u>Status</u>

On the basis of the findings to date, the annealing and reirradiation conditions for Experiments 3 and 4 were established at 399°C -168 hr and $\sim 7 \times 10^{18}$ n/cm^2 >1 MeV (ϕ^{cs}), respectively. Reactor operations required for Experiments 3A through 3C and Experiments 4A through 4C subsequently have been completed, and postirradiation testing operations have commenced. Experiments 3D and 3E and Experiments 4D and 4E presently are undergoing their second cycle irradiation exposure.

III. FRACTURE MECHANICS INVESTIGATION

A. J Integral Characterization of Low Upper Shelf A302-B Steel Plate

F.J. Loss, R.A. Gray, Jr., and B.H. Menke

Background

A program is being conducted to characterize the fracture toughness of pressure vessel steels that exhibit a lower upper shelf energy. This investigation has been motivated by the projected drop in the Charpy-V (C_V) upper shelf energy to levels less than 68J (50 ft-lb), caused by irradiation of steels used in the construction of certain older LWR pressure vessels. It is necessary to characterize the toughness in terms of fracture mechanics to permit an assessment to be made of the margin of safety against fracture associated with a given C_V upper shelf energy. However, it is difficult to measure the toughness of these irradiated steels with linear elastic fracture mechanics (LEFM) techniques because of the large sizes of irradiated specimens that may be required. While it is feasible to irradiate smaller specimens, e.g. 25 mm thick, these specimens are expected to exhibit an elastic-plastic behavior. For tests of this type, the J integral R-curve approach is being applied to characterize the low shelf alloys and also to permit an assessment to be made of full-section behavior using small specimens.

The current ASTM-recommended method for J_{Ic} measurement requires several specimens to be tested in which the crack extension (Δa) may be determined by "heat tinting" and measuring the fracture surface. Because of the difficulties in obtaining and testing irradiated specimens, it is necessary to develop a single specimen techique for the assessment of both J_{Ic} and the R curve. Current emphasis has been to develop the unloading compliance method (UCM) as a viable single specimen J technique for application to irradiated CT specimens.

Investigations have centered on an A302-B steel having an upper shelf energy of approximately 68J. The melt for this plate was specially selected and processed to provide a representative pressure vessel steel that could be used to assess the toughness associated with the 68J C_V energy level. The latter energy is the lowest value permitted by Appendix G of 10 CFR Part 50 without the necessity for complete volumetric inspection of the beltline region and a fracture mechanics analysis to demonstrate adequate margins for continued operations.

The primary objective in the current phase of the program is to develop the UCM to a point where it can be used to predict the J-R curve obtained from the multispecimen heat-tint technique. In the next phase, this method will be applied in the assessment of irradiated specimens of the IAR program (see Sec. II of this report).

Other current objectives are to characterize the influence of face grooves as well as the effects of specimen size on the J-R curve. In addition, a cooperative program was initiated between CISE (Italy) and NRL. The objectives of that program are (a) to obtain an inter-laboratory comparison of the J-R curves for the A302-B steel using the heat tint technique, and (b) to investigate size effects with CT specimens of 12.5 25, and 50-mm thickness.

Unloading Compliance Method Development

The successful application of the UCM rests in the elimination of frictional effects in the mechanical apparatus so as to minimize the hysteresis obtained in the record of load (P) vs load-line deflection (δ). It is also necessary to employ electronics that are capable of resolving the small signals obtained from the load and displacement transducers.

The current investigation employs a 1TCT specimen (Fig. 9) having a modified notch and pin-hole spacing to permit the placement of razor knife edges on the load line. The use of knife edges in conjunction with a clip gage decreases the hysteresis in the load vs displacement record. The interaction of the specimen grips and loading pins was also believed to influence the hysteresis. Fortunately, this area of concern was found to be inconsequential for the particular amplification employed of the load and deflection signals. Use of bearings in the grip pin holes as well as flat-bottom holes in the grips produced the same hysteresis as grips having a hole approximately equal to the pin diameter. Current testing is being conducted with a flat-bottom grips.

Specimen Compliance The compliance (δ/P) curves for both smooth and 25% face-grooved specimens were derived experimentally (Fig. 10) using 1TCT specimens as shown in Fig. 9. The data are presented in Table 4. Various crack length-to-width ratios were obtained by machining the notches to the desired depths. (The notch tip geometry was the same as that illustrated in Fig. 9). Each point in Fig. 10 represents an average of ten repetitive loadings. Two data points are shown for the face-grooved specimen at 200^{o}C. These points lie above the data at room temperature because of a small decrease in modulus ($\approx$5%) at the higher temperature.

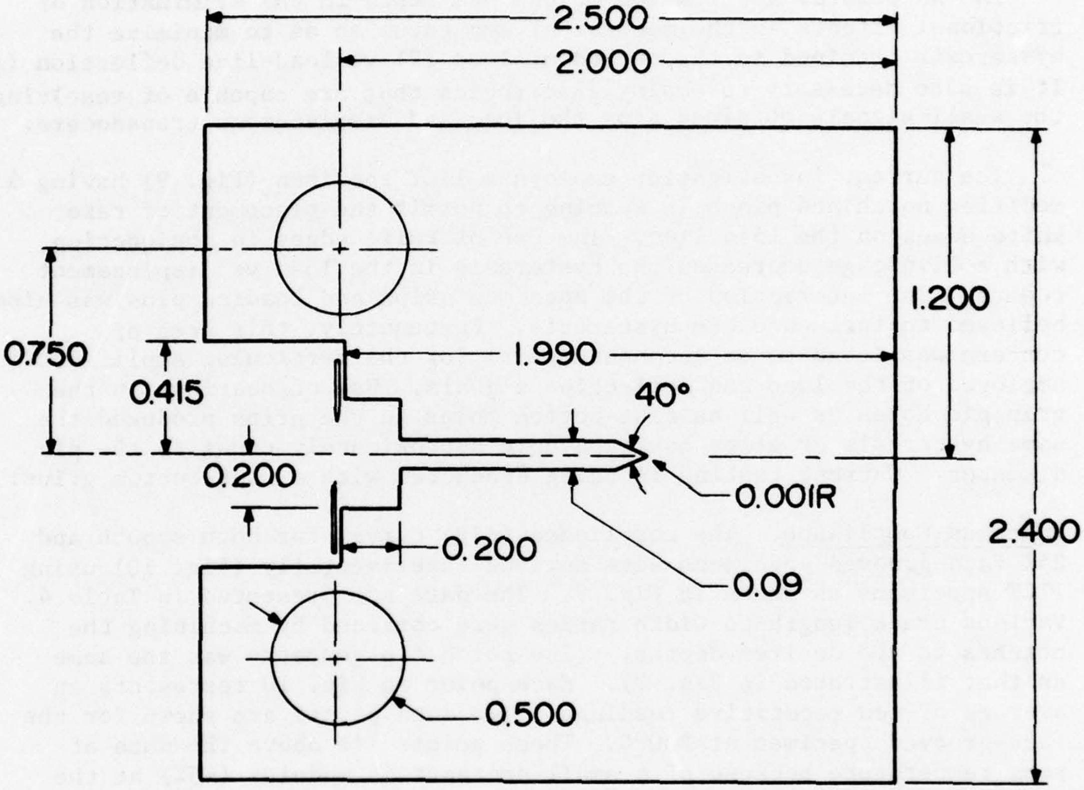

Fig. 9 - 1T specimen geometry for J_{Ic} testing. The ASTM standard design has been modified to permit a larger hole spacing and a different notch geometry to accommodate razor knife edges on this load line.

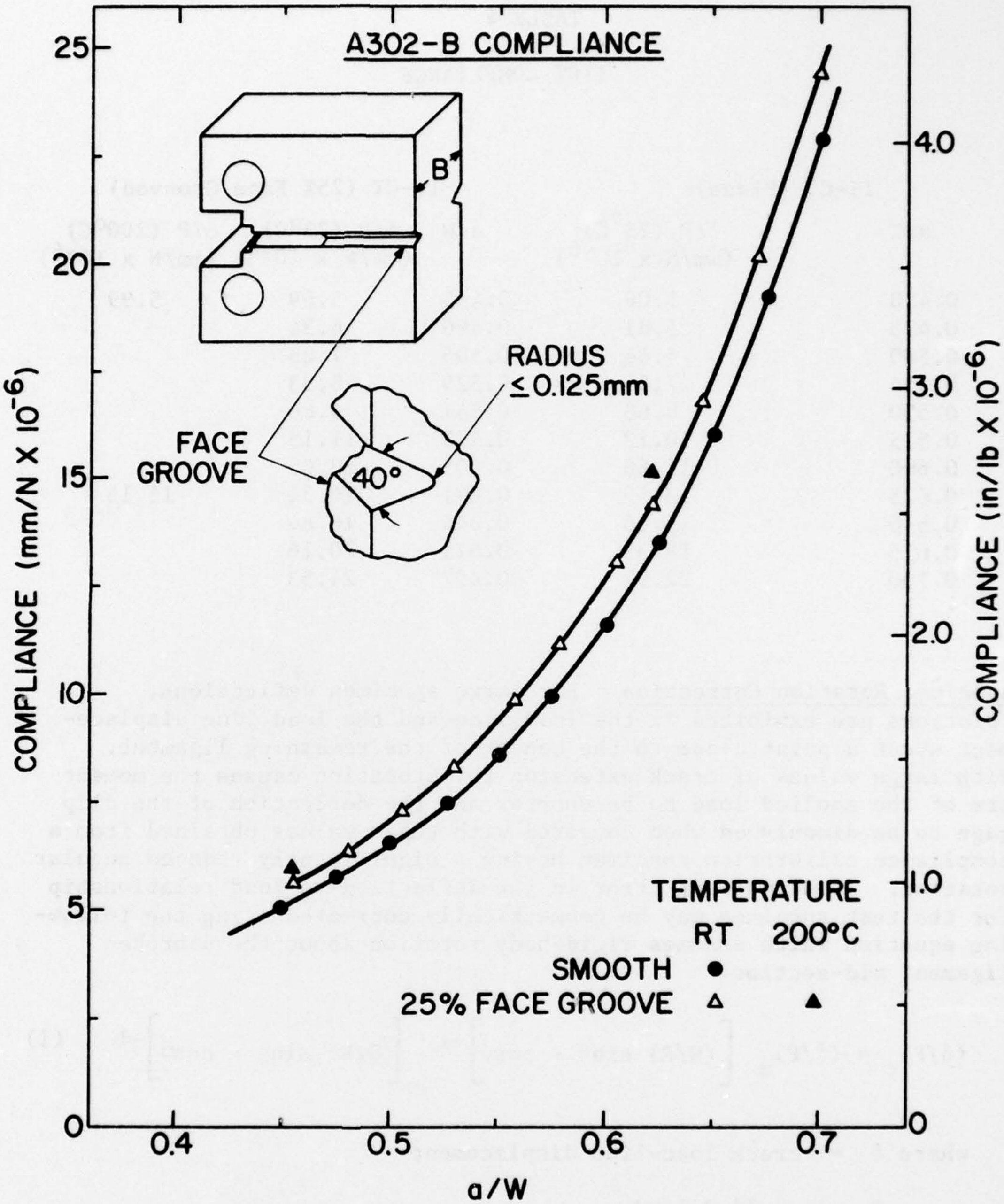

Fig. 10 - Experimentally determined compliance of plane and face-grooved specimens.

TABLE 4

1TCT COMPLIANCE

1T-CT (Plane)		1T-CT (25% Face Grooved)		
a/W	δ/P (23°C) (mm/N x 10^{-6})	a/W	δ/P (23°C) (mm/N x 10^{-6})	δ/P (200°C) (mm/N x 10^{-6})
0.450	5.06	0.455	5.69	5.99
0.475	5.81	0.480	6.34	
0.500	6.66	0.505	7.25	
0.524	7.56	0.529	8.33	
0.550	8.68	0.557	9.86	
0.575	10.12	0.578	11.15	
0.600	11.66	0.605	13.05	
0.625	13.59	0.621	14.31	15.15
0.650	16.06	0.644	16.84	
0.675	19.33	0.671	20.16	
0.700	22.92	0.697	24.53	

Specimen Rotation Correction For large specimen deflections, rotations are exhibited in the load line and the load line displacement about a point close to the center of the remaining ligament. With large values of crack extension this rotation causes the moment arm of the applied load to be shorter and the deflection of the clip gage to be dimenished when compared with those values obtained from a compliance calibration specimen having a significantly reduced angular rotation. This inherent error in the deflection-vs-load relationship for the test specimen may be geometrically corrected using the following equation which assumes rigid-body rotation about the unbroken ligament mid-section:

$$(\delta/P)_c = (\delta/P)_m \left[(H/R)\sin\theta - \cos\theta\right]^{-1} \left[(D/R)\sin\theta - \cos\theta\right]^{-1} \quad (1)$$

where δ = crack load-line displacement

P = applied load

c = corrected for rotation

m = measured experimentally

H = half span of applied load points

R = radius of rotation of crack centerline at measurement line assuming a plastic hinge about the center of uncracked ligament

D = distance from crack plane to measurement line when $P = 0$

θ = angle of rotation of rigid body element about unbroken mid-section line

w = width of specimen

a = crack length from load plane

$$R = \frac{W-a}{2}$$

$$\theta = \sin^{-1}\left[(\delta_m + D) \Big/ (D^2 + R^2)^{0.5}\right] - \tan^{-1}(D/R)$$

The above terms are illustrated in Fig. 11.

The ratio of corrected and measured values of δ/P from Eq. (1) is graphically presented as a function of relative crack length (a/W) in Fig. 12. The corrections for this exact solution have been found to agree to within 0.3% of those given by the equation derived by Clark (5) over the range of conditions normally found in compact toughness J tests.

Application of UCM

During each test, two records of load vs load-line displacement are obtained. One record (Fig. 13) defines the complete loading history of the specimen, including the small ($\approx$10%) unloading at periodic intervals which is performed to determine the specimen compliance change. The unloading regions are greatly amplified (Fig. 14) to permit an accurate value of the slope $(\delta/P)^{-1}$ to be measured.

The applied J integral value at a given unloading (e.g., position 5 in Fig. 13) is determined from the relation

$$J = \frac{2A}{Bb} \tag{2}$$

where A is the area under the load vs deflection record, B is the specimen thickness and b is the original unbroken ligament measured from the fatigue precrack. This value of J is adjusted for the tension component in the CT specimen using the Merkle-Corten procedure (6).

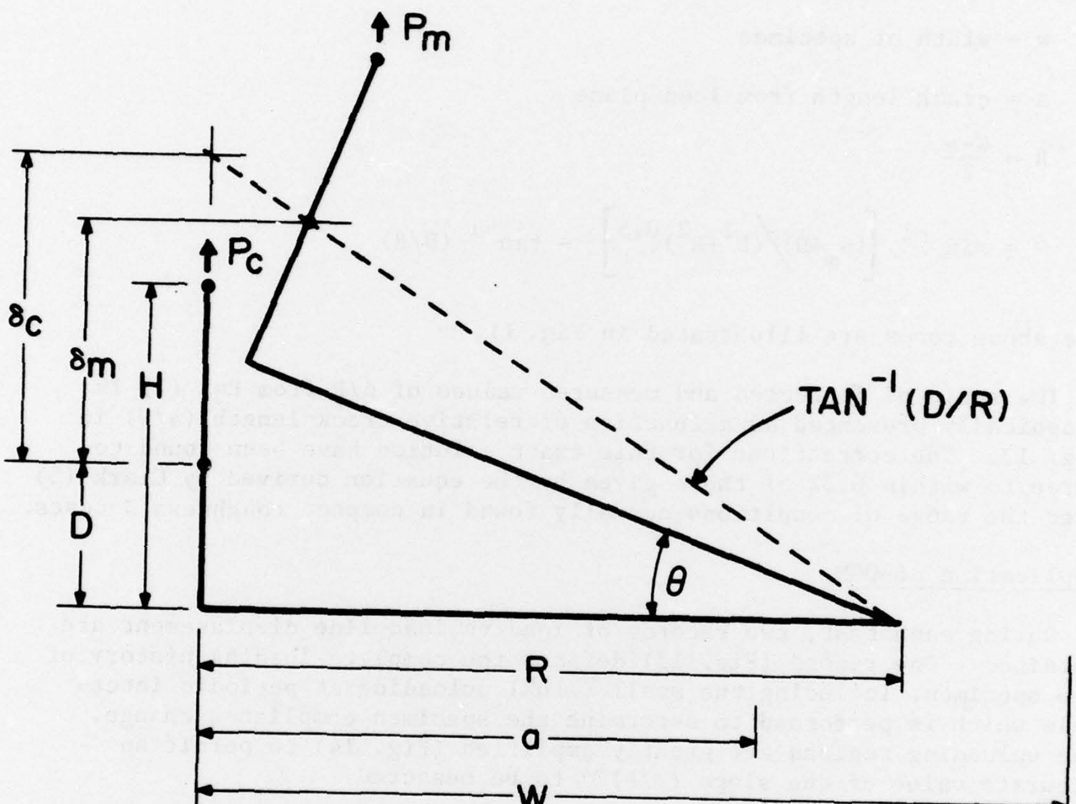

Fig. 11 - Schematic of elastic compliance correction for large specimen rotations.

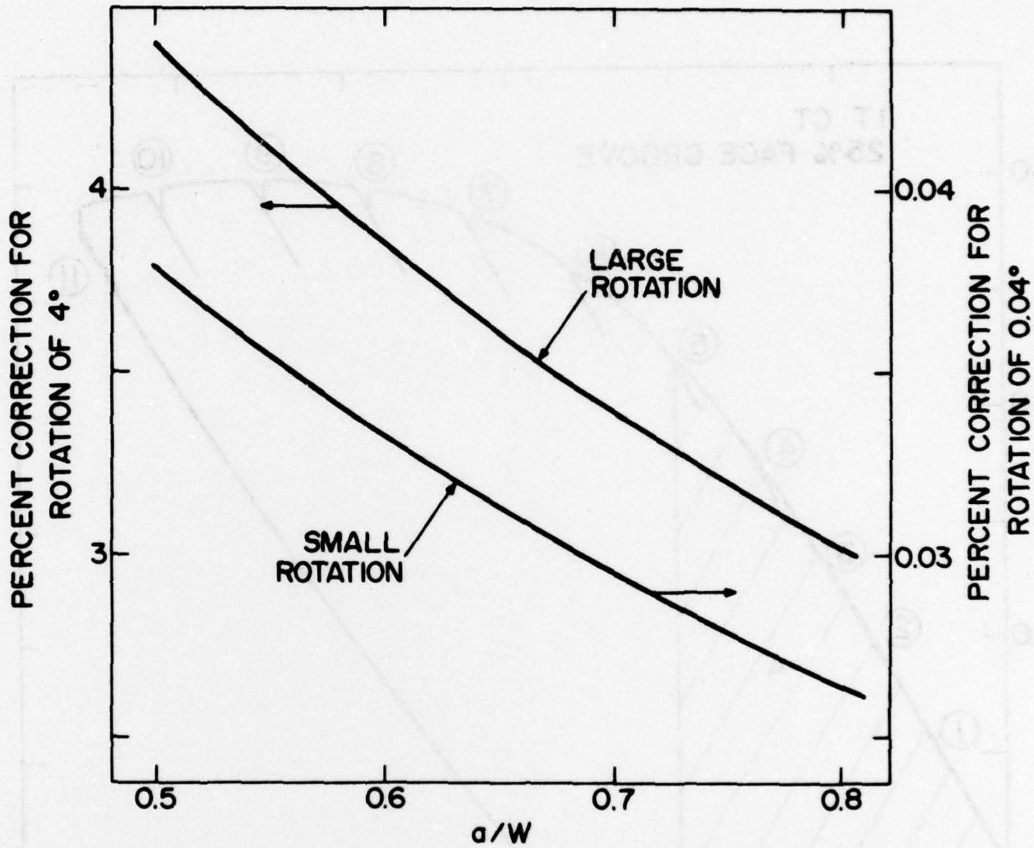

Fig. 12 - Compliance (δ/P) correction necessitated by specimen rotation (Eq. 1).

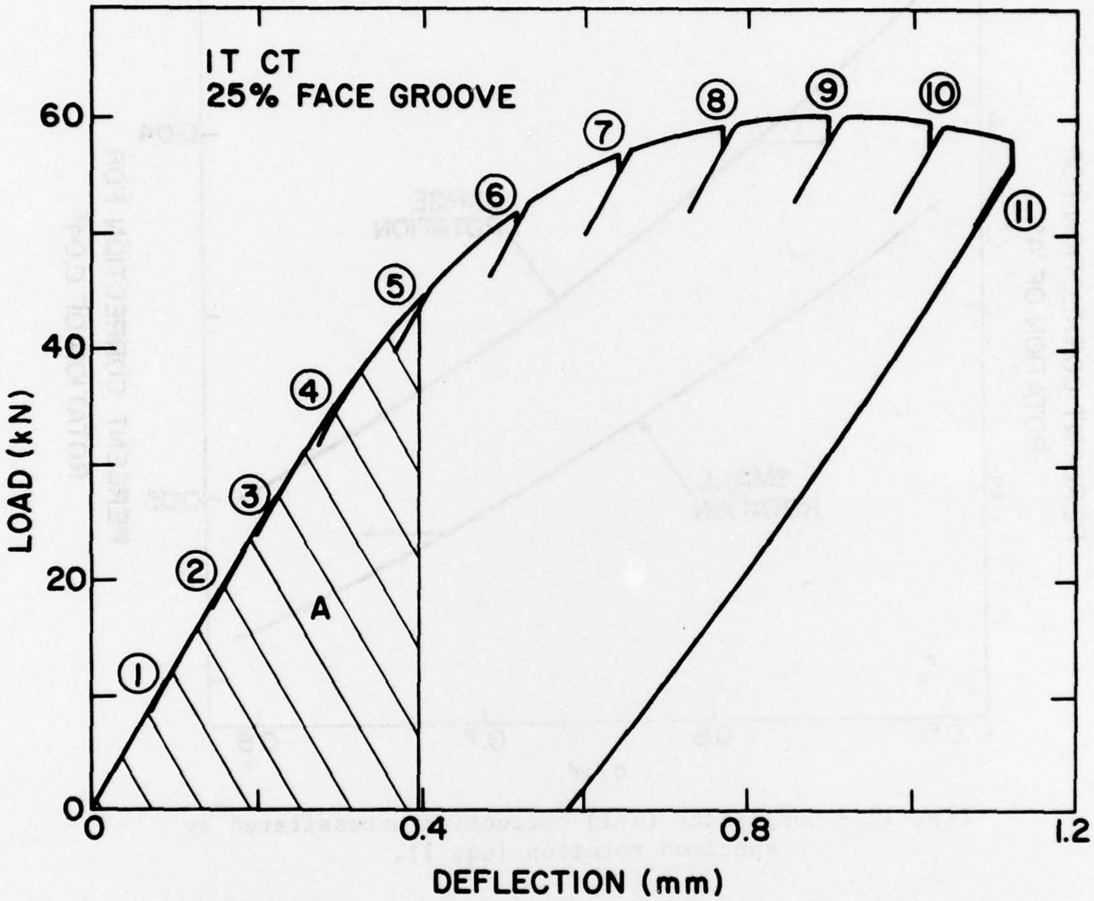

Fig. 13 - Typical load vs deflection record from a 1TCT specimen illustrating the periodic unloadings performed to assess the crack extension. The area A is used in conjunction with Eq. 2 to compute the applied J level at a particular unloading.

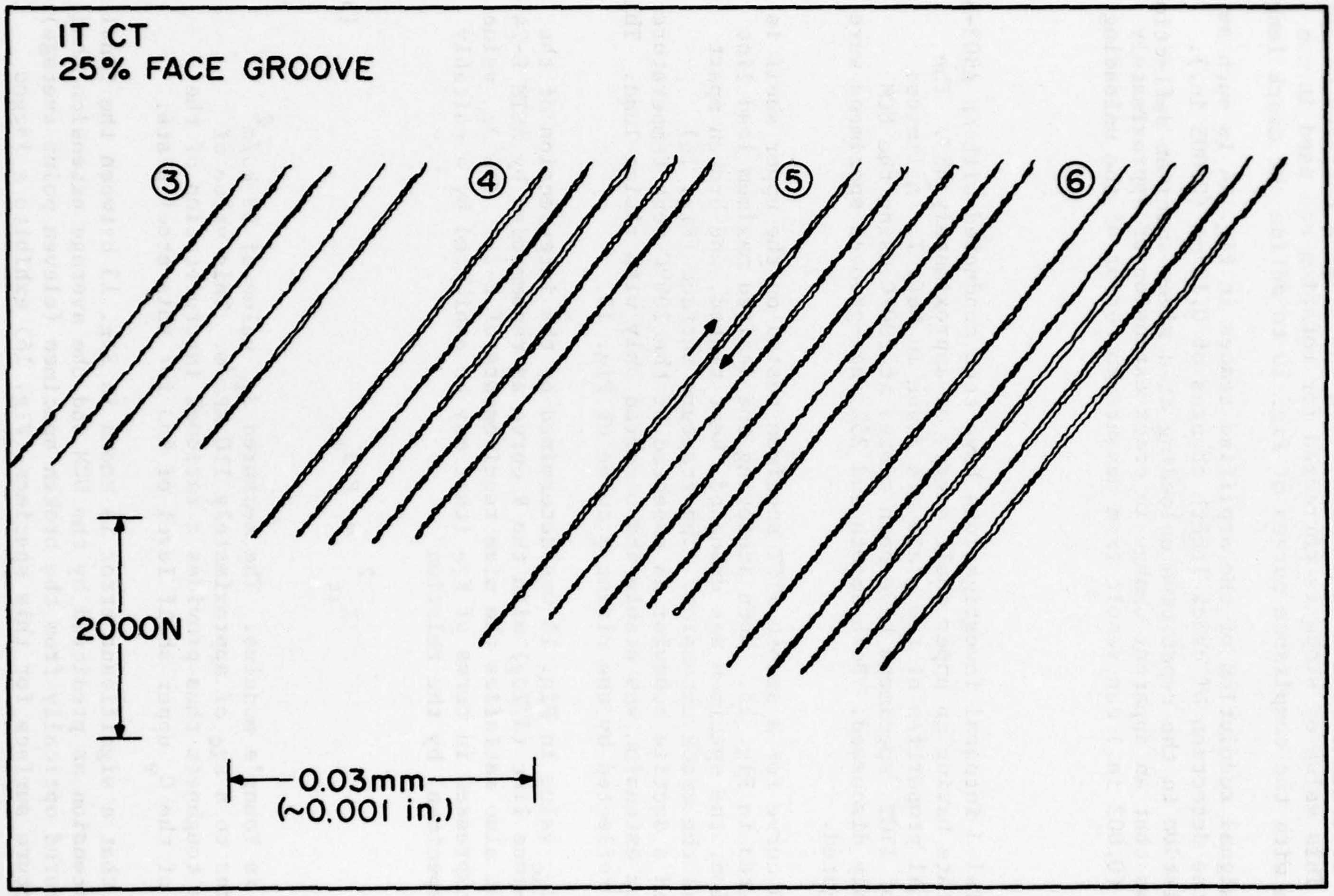

Fig. 14 - Amplification of the unloading traces shown in Fig. 13. Several unloadings are performed at a given specimen deflection to determine an average value of compliance.

Repetitive unloadings are produced at a given specimen deflection to permit an average slope to be determined (Fig. 14). These amplified traces are quite linear and exhibit little hysteresis. Consequently, the slope is determined from both the unloading and loading portions of the trace. This value of slope is corrected for rotation and used in conjunction with the compliance curves of Fig. 10 to define the crack length.

The signal resolution of the amplified traces in Fig. 14 is such as permit the detection of crack length changes of 0.13 mm (0.005 in.). The variation in the repetitive unloading at a given specimen deflection has shown that an apparent change in crack extension of approximately 0.05 mm (0.002 in.) can result from measurement error of the unloading slope.

Results

Initial J integral investigations have been conducted with an A302-B steel plate having an upper shelf energy of approximately 68J. The mechanical properties of the plate are given in Ref. 7. A limited number of 1TCT specimens have been tested at 200°C using the UCM previously discussed. Both smooth and 25% face-grooved specimens were investigated.

A J-R curve for a smooth 1TCT specimen tested on the upper shelf is illustrated in Fig. 15. Upon achieving the desired maximum load line deflection, the specimen was unloaded, heat tinted, and broken apart to reveal the crack extension. The fracture surface (Fig. 16) exhibited a ductile behavior as expected at the 200°C test temperature. The crack extension was stable and occurred only with rising load. This fact is reflected by the rising R curve of Fig. 15.

The J_{Ic} value in Fig. 14 was determined by the intersection of the stretch-zone line ($J/2\sigma_f$) with the R curve as recommended by ASTM E-24. This test also satisfies the size requirements of E-24. The J_{Ic} value can be expressed in terms of K_{Ic} (that may be exhibited by a suitably larger specimen) by the relation

$$K_{Ic}^2 = E\,J_{Ic} \qquad (3)$$

where E is Young's modulus. The measured J_{Ic} value of 59 kJ/m^2 translates to a K_{Ic} of approximately 110 MPa$\sqrt{m}$. This value of fracture toughness thus provides a rational interpretation of the meaning of the C_v upper shelf level of 68J for this steel plate.

Note that a significant error is shown in Fig. 15 between the final crack extension as predicted by the UCM and the average extension that was measured optically from the broken specimen (eleven point average). The fracture surface for this specimen (Fig. 16) exhibits a jagged

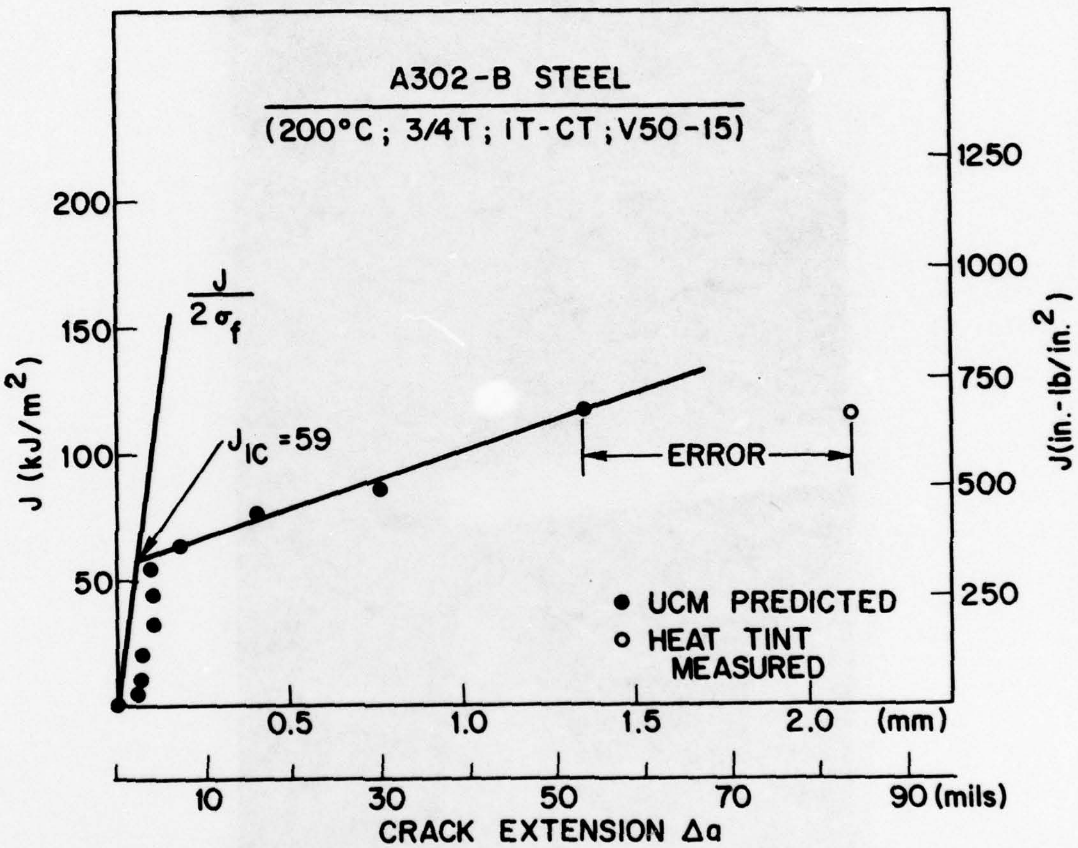

Fig. 15 - Illustration of the J-R curve obtained by the UCM. The test was conducted in the upper shelf region and the crack extension occurred in a ductile manner. The "measured" value of Δa was determind optically from the heat tinted fracture surface.

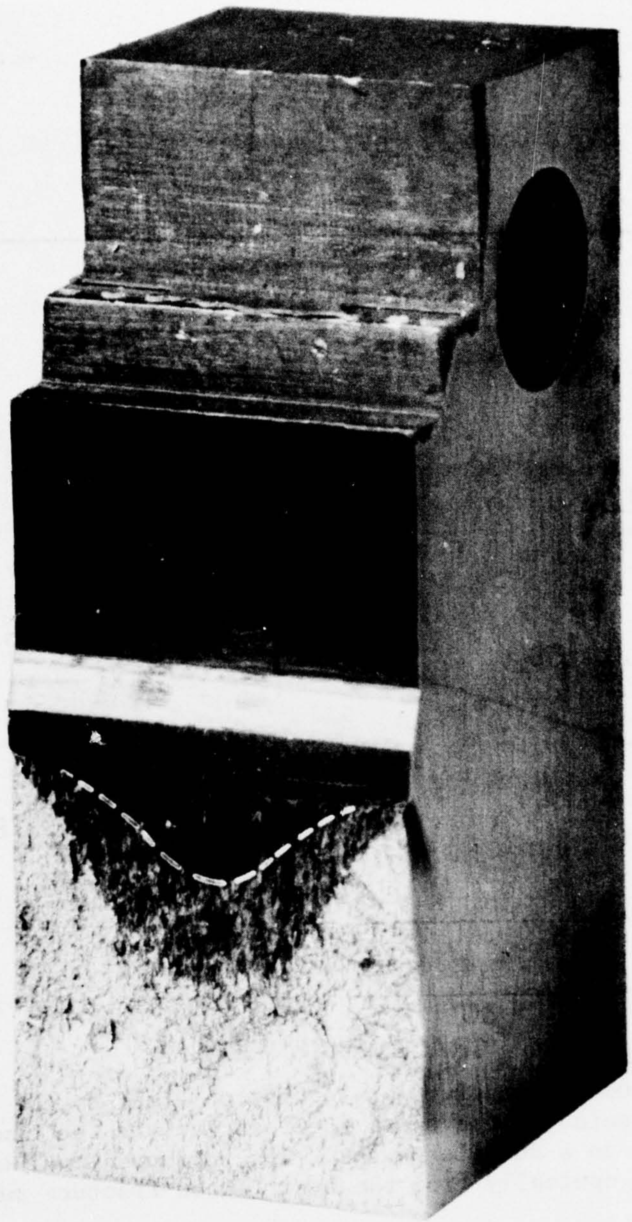

Fig. 16 - Fracture surface associated with the J-R curve in Fig. 15. The heat tinted crack extension defined by the "measured" point in Fig. 15 has been outlined. The larger thumbnail marking of the fracture surface was produced by a second loading of the specimen.

front that presents some difficulty in optical measurement. These crack front irregularities were visually averaged to define the stated crack extension. In spite of potential inaccuracies in the visual crack length determination, this phenomenon is not believed to account for the error illustrated in Fig. 16.

It was postulated that the error between visual and UCM crack extension measurements could result from the tunneling of the crack front in the smooth specimen. Recall that the specimen compliance was determined with a straight crack front. Consequently, specimens having 25% face grooves were investigated. The face grooving did produce a straight, but still jagged, crack front as illustrated in Fig. 17. However, the J-R curve for this specimen (Fig. 18) also exhibits an error between optical and UCM determinations of crack extension. The source of the error is currently unresolved.

Note that there is a good agreement of the J_{Ic} values between smooth and face-grooved specimens (Fig. 15 vs Fig. 18). This correspondence may be fortuitous in that other tests have indicated a larger spread in J_{Ic} values. Also note that the slope of R curve for the face-grooved specimen is less than that for the smooth specimen. This observation suggests that the R-curve slope may be dependent upon specimen geometry. Provided this apparent geometry dependence is verified through additional testing, it could be concluded that conservative definition of the material fracture behavior may require additional emphasis on the use of face-grooved specimens.

Fig. 17 - Fracture surface of a specimen that has been face-grooved. This specimen illustrates **the crack front shape at two points in the loading history (indicated by arrows). Face grooving effectively eliminates the crack-front curvature that was illustrated in Fig. 16.**

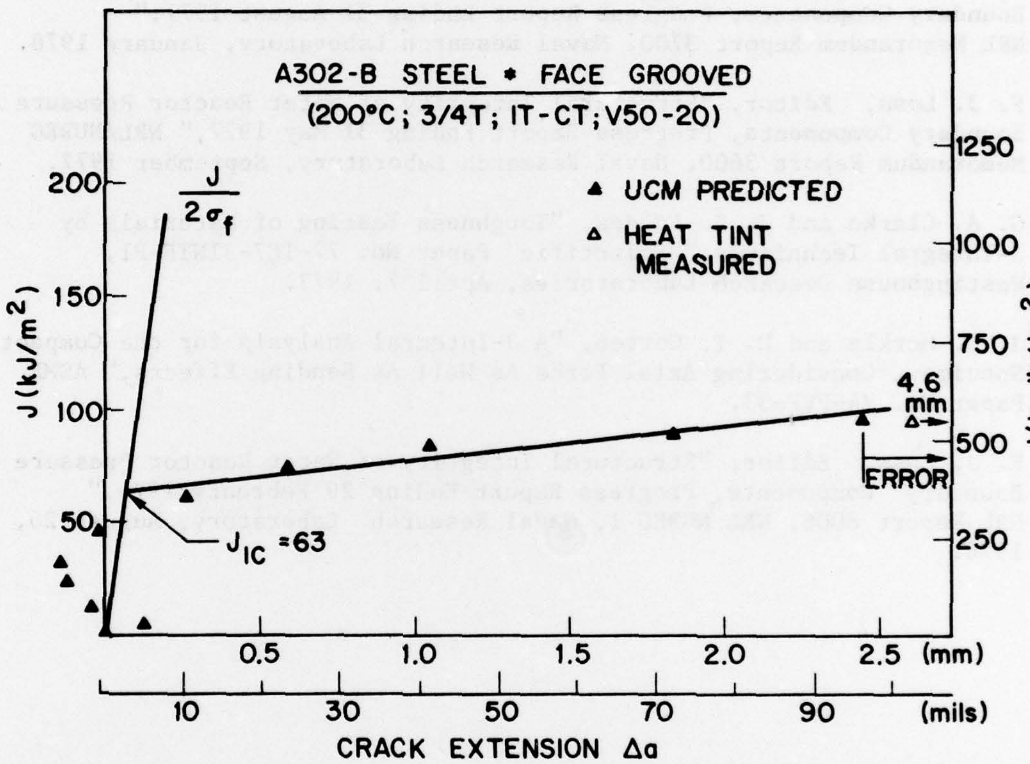

Fig. 18 - J-R curve obtained from a face-grooved specimen. Note that the measured value of crack extension from the heat tinted surface does not agree with the value predicted by the UCM.

REFERENCES

1. W. G. Clark, Jr. and S. J. Hudak, Jr., "Variability in Fatigue Crack Growth Rate Testing," Scientific Paper No. 74-1E7-MSLRA-P2, Westinghouse Research Laboratories, September 18, 1974.

2. F. J. Loss, Editor, "Structural Integrity of Water Reactor Pressure Boundary Components, Progress Report Ending 28 February 1977," NRL/NUREG Memorandum Report 3512, Naval Research Laboratory, May 1977.

3. F. J. Loss, Editor, "Structural Integrity of Water Reactor Pressure Boundary Components, Progress Report Ending 31 August 1977," NRL Memorandum Report 3700, Naval Research Laboratory, January 1978.

4. F. J. Loss, Editor, "Structural Integrity of Water Reactor Pressure Boundary Components, Progress Report Ending 31 May 1977," NRL/NUREG Memorandum Report 3600, Naval Research Laboratory, September 1977.

5. G. A. Clarke and J. D. Landes, "Toughness Testing of Materials by J-Integral Techniques," Scientific Paper No. 77-1E7-JINTF-P1, Westinghouse Research Laboratories, April 7, 1977.

6. J. G. Merkle and H. T. Corten, "A J-Integral Analysis for the Compact Specimen, Considering Axial Force As Well As Bending Effects," ASME Paper No. 74-PVP-33.

7. F. J. Loss, Editor, "Structural Integrity of Water Reactor Pressure Boundary Components, Progress Report Ending 29 February 1976," NRL Report 8006, NRL NUREG 1, Naval Research Laboratory, August 26, 1976.